arXiv:1507.06732v2 [hep-ph] 14 Nov 2015

Lepton flavor violation in the BLMSSM

Shu-Min Zhao[1]*, Tai-Fu Feng[1,2]†, Hai-Bin Zhang[1], Xi-Jie Zhan[1], Yin-Jie Zhang[1], Ben Yan[1]

[1] *Department of Physics, Hebei University, Baoding 071002, China*

[2] *State Key Laboratory of Theoretical Physics, Institute of Theoretical Physics, Chinese Academy of Sciences, Beijing 100190, China*

(Dated: November 17, 2015)

Abstract

In a supersymmetric extension of the standard model with local gauged baryon and lepton numbers (BLMSSM), there are new sources for lepton flavor violation, because the right-handed neutrinos and new gauginos are introduced. In BLMSSM, we study the charged lepton flavor violating processes $l_j \to l_i + \gamma$ and $l_j \to 3l_i$ in detail. The numerical results show that in some parameter space the branching ratios for charged lepton flavor violating processes can be large enough to be detected in the near future.

PACS numbers: 11.15Ex, 11.30Pb, 14.60-z

Keywords: Supersymmetric, Lepton flavor violation, BLMSSM

---

* zhaosm@hbu.edu.cn

† fengtf@hbu.edu.cn

I. INTRODUCTION

From the neutrino oscillation experiments[1], it is convincing that neutrinos have tiny masses and mix with each other[2, 3]. Therefore, lepton flavor symmetry is not exact in the universe. Though the standard model(SM) has achieved great success with the detected lightest CP-even Higgs, SM should be extended. Because of the GIM mechanism, in SM the charged lepton flavor violating(CFLV) processes are very tiny, for example $Br_{SM}(l_j \to l_i + \gamma) \sim 10^{-55}$[4]. The experiment upper bounds of the CLFV processes $l_j \to l_i + \gamma$ and $l_j \to 3l_i$ are[5]

$$\begin{aligned}
&\mathtt{Br}(\mu \to e\gamma) < 5.7 \times 10^{-13}, \qquad \mathtt{Br}(\mu \to 3e) < 1.0 \times 10^{-12}, \\
&\mathtt{Br}(\tau \to e\gamma) < 3.3 \times 10^{-8}, \qquad \mathtt{Br}(\tau \to \mu\gamma) < 4.4 \times 10^{-8}, \\
&\mathtt{Br}(\tau \to 3e) < 2.7 \times 10^{-8}, \qquad \mathtt{Br}(\tau \to 3\mu) < 2.1 \times 10^{-8}. \qquad (1)
\end{aligned}$$

They are much larger than the corresponding SM theoretical predictions. To explore new physics beyond SM, study CLFV processes is an effective approach. Once physicists observe CLFV processes in future experiments, there must be new physics beyond SM.

In a simple extension of SM, with a new additional Yukawa matrix for right-handed neutrinos, CLFV processes are induced at loop level with neutrino[6]. They are suppressed strong by the tiny neutrino masses and impossible to be observed practically. One popular supersymmetric extension of SM is the minimal suppersymmetric standard model(MSSM)[7]. In R-parity conserved MSSM, the left-handed light neutrinos are still massless and can not explain the discovery of neutrino oscillations. Therefore, physicists extend MSSM to account for the light neutrino masses and mixings. Adding low-scale right-handed neutrinos and approximate lepton number symmetries, ν_RMSSM is obtained, where the authors study the CLFV processes[8]. In the supersymmetric standard model with right-handed neutrino supermultiplets, the authors investigate various LFV processes in detail[9]. In our previous work, we study neutrino masses and CLFV processes in $\mu\nu$SSM[10].

For the beyond SM models, one can violate R parity[11] with the non-conservation of baryon number (B) or lepton number (L)[12, 13]. A minimal supersymmetric extension of the SM with local gauged B and L(BLMSSM) is a favorite one[14]. BLMSSM was first proposed in one of the references in [14]. In the work, this model is that we are adopting. The local gauged B is used to explain the matter-antimatter asymmetry in the universe.

Right-handed neutrinos are introduced in BLMSSM to account for the neutrino oscillation experiments, which lead to three tiny neutrino masses through the seesaw mechanism. Then lepton number (L) is expected to be broken spontaneously around TeV scale. In BLMSSM, the lightest CP-even Higgs mass and the decays $h^0 \to \gamma\gamma$, $h^0 \to ZZ(WW)$ are studied in the work[15]. Taking into account the Yukawa couplings between Higgs and exotic quarks, we study the neutron and lepton electric dipole moments(EDMs) in the CP-violating BLMSSM[16, 17]. $B^0 - \bar{B}^0$ mixing and $t \to c + \gamma, t \to c + g$ are also investigated in SM extension with local gauged baryon and lepton numbers[18].

In this work, we analyze these CLFV processes ($\mu \to e\gamma$, $\mu \to 3e$; $\tau \to e\gamma$, $\tau \to \mu\gamma$, $\tau \to 3e$,$\tau \to 3\mu$) in the frame work of BLMSSM. Compared with MSSM, there are new sources to enlarge these CLFV processes via loop contributions. The new CLFV scores are produced from 1. the right-handed neutrinos mixing with left-handed neutrinos; 2. the coupling of new neutralino(lepton neutralino)-slepton-lepton. In some parameter space of BLMSSM, large corrections to the CLFV processes are obtained, and can easily exceed their experiment upper bounds. Therefore, to enhance these CLFV processes is possible, and they may be measured in the near future.

After this introduction, we briefly summarize the main ingredients of the BLMSSM, and show the needed mass matrices and couplings in section 2. In section 3, the decay widths of these interested CLFV processes are analyzed. The input parameters and numerical analysis are shown in section 4 and we give our conclusion in section 5.

II. BLMSSM

BLMSSM is the supersymmetric extension of the SM with local gauged B and L, whose local gauge group is $SU(3)_C \otimes SU(2)_L \otimes U(1)_Y \otimes U(1)_B \otimes U(1)_L$[12]. The exotic leptons $\hat{L}_4 \sim (1,\ 2,\ -1/2,\ 0,\ L_4)$, $\hat{E}_4^c \sim (1,\ 1,\ 1,\ 0,\ -L_4)$, $\hat{N}_4^c \sim (1,\ 1,\ 0,\ 0,\ -L_4)$, $\hat{L}_5^c \sim (1,\ 2,\ 1/2,\ 0,\ -(3 + L_4))$, $\hat{E}_5 \sim (1,\ 1,\ -1,\ 0,\ 3 + L_4)$ and $\hat{N}_5 \sim (1,\ 1,\ 0,\ 0,\ 3 + L_4)$ are introduced to cancel L anomaly. As well as, the exotic quarks $\hat{Q}_4 \sim (3,\ 2,\ 1/6,\ B_4,\ 0)$, $\hat{U}_4^c \sim (\bar{3},\ 1,\ -2/3,\ -B_4,\ 0)$, $\hat{D}_4^c \sim (\bar{3},\ 1,\ 1/3,\ -B_4,\ 0)$, $\hat{Q}_5^c \sim (\bar{3},\ 2,\ -1/6,\ -(1 + B_4),\ 0)$, $\hat{U}_5 \sim (3,\ 1,\ 2/3,\ 1 + B_4,\ 0)$ and $\hat{D}_5 \sim (3,\ 1,\ -1/3,\ 1 + B_4,\ 0)$ are introduced to cancel B anomaly. To break lepton number and baryon number spontaneously, the Higgs superfields $\hat{\Phi}_L(1, 1, 0, 0, -2), \hat{\varphi}_L(1, 1, 0, 0, 2)$ and $\hat{\Phi}_B(1, 1, 0, 1, 0), \hat{\varphi}_B(1, 1, 0, -1, 0)$ are introduced respectively. Now, Higgs mechanism is the very massy foundtion stone for particle physics, and people are convinced of it, because of the detection of the lightest CP even Higgs h^0 at LHC[19]. The Higgs fields $\hat{\Phi}_L, \hat{\varphi}_L$ and $\hat{\Phi}_B, \hat{\varphi}_B$ acquire nonzero vacuum expectation values (VEVs), then exotic leptons and exotic quarks obtain masses. In the BLMSSM, the superfields $\hat{X}(1,1,0,2/3+B_4,0)$, $\hat{X}'(1,1,0,-(2/3+B_4),0)$ are introduced to make the heavy exotic quarks unstable. Furthermore $\hat{X}$ and $\hat{X}'$ mix together, where the lightest mass eigenstate can be a candidate for dark matter.

The superpotential of BLMSSM is[15]

$$\begin{aligned}
&\mathcal{W}_{BLMSSM} = \mathcal{W}_{MSSM} + \mathcal{W}_B + \mathcal{W}_L + \mathcal{W}_X \;, \\
&\mathcal{W}_B = \lambda_Q \hat{Q}_4 \hat{Q}_5^c \hat{\Phi}_B + \lambda_U \hat{U}_4^c \hat{U}_5 \hat{\varphi}_B + \lambda_D \hat{D}_4^c \hat{D}_5 \hat{\varphi}_B + \mu_B \hat{\Phi}_B \hat{\varphi}_B \\
&\qquad + Y_{u_4} \hat{Q}_4 \hat{H}_u \hat{U}_4^c + Y_{d_4} \hat{Q}_4 \hat{H}_d \hat{D}_4^c + Y_{u_5} \hat{Q}_5^c \hat{H}_d \hat{U}_5 + Y_{d_5} \hat{Q}_5^c \hat{H}_u \hat{D}_5 \;, \\
&\mathcal{W}_L = Y_{e_4} \hat{L}_4 \hat{H}_d \hat{E}_4^c + Y_{\nu_4} \hat{L}_4 \hat{H}_u \hat{N}_4^c + Y_{e_5} \hat{L}_5^c \hat{H}_u \hat{E}_5 + Y_{\nu_5} \hat{L}_5^c \hat{H}_d \hat{N}_5 \\
&\qquad + Y_\nu \hat{L} \hat{H}_u \hat{N}^c + \lambda_{N^c} \hat{N}^c \hat{N}^c \hat{\varphi}_L + \mu_L \hat{\Phi}_L \hat{\varphi}_L \;, \\
&\mathcal{W}_X = \lambda_1 \hat{Q} \hat{Q}_5^c \hat{X} + \lambda_2 \hat{U}^c \hat{U}_5 \hat{X}' + \lambda_3 \hat{D}^c \hat{D}_5 \hat{X}' + \mu_X \hat{X} \hat{X}' \;. \qquad (2)
\end{aligned}$$

where $\mathcal{W}_{MSSM}$ is the superpotential of the MSSM. The soft breaking terms $\mathcal{L}_{soft}$ of the BLMSSM can be found in the works[14, 15]

$$\begin{aligned}
\mathcal{L}_{soft} = \;& \mathcal{L}_{soft}^{MSSM} - (m^2_{\tilde{N}^c})_{IJ} \tilde{N}_I^{c*} \tilde{N}_J^c - m^2_{\tilde{Q}_4} \tilde{Q}_4^\dagger \tilde{Q}_4 - m^2_{\tilde{U}_4} \tilde{U}_4^{c*} \tilde{U}_4^c - m^2_{\tilde{D}_4} \tilde{D}_4^{c*} \tilde{D}_4^c \\
& - m^2_{\tilde{Q}_5} \tilde{Q}_5^{c\dagger} \tilde{Q}_5^c - m^2_{\tilde{U}_5} \tilde{U}_5^* \tilde{U}_5 - m^2_{\tilde{D}_5} \tilde{D}_5^* \tilde{D}_5 - m^2_{\tilde{L}_4} \tilde{L}_4^\dagger \tilde{L}_4 - m^2_{\tilde{\nu}_4} \tilde{N}_4^{c*} \tilde{N}_4^c \\
& - m^2_{\tilde{e}_4} \tilde{E}_4^{c*} \tilde{E}_4^c - m^2_{\tilde{L}_5} \tilde{L}_5^{c\dagger} \tilde{L}_5^c - m^2_{\tilde{\nu}_5} \tilde{N}_5^* \tilde{N}_5 - m^2_{\tilde{e}_5} \tilde{E}_5^* \tilde{E}_5 - m^2_{\Phi_B} \Phi_B^* \Phi_B \\
& - m^2_{\varphi_B} \varphi_B^* \varphi_B - m^2_{\Phi_L} \Phi_L^* \Phi_L - m^2_{\varphi_L} \varphi_L^* \varphi_L - \Big(m_B \lambda_B \lambda_B + m_L \lambda_L \lambda_L + h.c. \Big) \\
& + \Big\{ A_{u_4} Y_{u_4} \tilde{Q}_4 H_u \tilde{U}_4^c + A_{d_4} Y_{d_4} \tilde{Q}_4 H_d \tilde{D}_4^c + A_{u_5} Y_{u_5} \tilde{Q}_5^c H_d \tilde{U}_5 + A_{d_5} Y_{d_5} \tilde{Q}_5^c H_u \tilde{D}_5 \\
& + A_{BQ} \lambda_Q \tilde{Q}_4 \tilde{Q}_5^c \Phi_B + A_{BU} \lambda_U \tilde{U}_4^c \tilde{U}_5 \varphi_B + A_{BD} \lambda_D \tilde{D}_4^c \tilde{D}_5 \varphi_B + B_B \mu_B \Phi_B \varphi_B + h.c. \Big\} \\
& + \Big\{ A_{e_4} Y_{e_4} \tilde{L}_4 H_d \tilde{E}_4^c + A_{\nu_4} Y_{\nu_4} \tilde{L}_4 H_u \tilde{N}_4^c + A_{e_5} Y_{e_5} \tilde{L}_5^c H_u \tilde{E}_5 + A_{\nu_5} Y_{\nu_5} \tilde{L}_5^c H_d \tilde{N}_5 \\
& + A_N Y_\nu \tilde{L} H_u \tilde{N}^c + A_{N^c} \lambda_{N^c} \tilde{N}^c \tilde{N}^c \varphi_L + B_L \mu_L \Phi_L \varphi_L + h.c. \Big\} \\
& + \Big\{ A_1 \lambda_1 \tilde{Q} \tilde{Q}_5^c X + A_2 \lambda_2 \tilde{U}^c \tilde{U}_5 X' + A_3 \lambda_3 \tilde{D}^c \tilde{D}_5 X' + B_X \mu_X X X' + h.c. \Big\} \;. \qquad (3)
\end{aligned}$$

The $SU(2)_L$ doublets $H_u,\ H_d$ should obtain nonzero VEVs $\upsilon_u,\ \upsilon_d$,

$$H_u = \begin{pmatrix} H_u^+ \\ \frac{1}{\sqrt{2}}\Big(\upsilon_u + H_u^0 + i P_u^0\Big) \end{pmatrix} \;, \qquad H_d = \begin{pmatrix} \frac{1}{\sqrt{2}}\Big(\upsilon_d + H_d^0 + i P_d^0\Big) \\ H_d^- \end{pmatrix} \;. \qquad (4)$$

The $SU(2)_L$ singlets Φ_B, φ_B obtain nonzero VEVs υ_B, $\overline{\upsilon}_B$,

$$\Phi_B = \frac{1}{\sqrt{2}}\Big(\upsilon_B + \Phi_B^0 + iP_B^0\Big) , \qquad \varphi_B = \frac{1}{\sqrt{2}}\Big(\overline{\upsilon}_B + \varphi_B^0 + i\overline{P}_B^0\Big) . \tag{5}$$

In the same way, the $SU(2)_L$ singlets Φ_L, φ_L obtain nonzero VEVs υ_L, $\overline{\upsilon}_L$,

$$\Phi_L = \frac{1}{\sqrt{2}}\Big(\upsilon_L + \Phi_L^0 + iP_L^0\Big) , \qquad \varphi_L = \frac{1}{\sqrt{2}}\Big(\overline{\upsilon}_L + \varphi_L^0 + i\overline{P}_L^0\Big) . \tag{6}$$

Therefore, the local gauge symmetry $SU(2)_L \otimes U(1)_Y \otimes U(1)_B \otimes U(1)_L$ breaks down to the electromagnetic symmetry $U(1)_e$.

$H^\pm = -\sin\beta H_d^\pm + \cos\beta H_u^\pm$ represent the charged Higgs, whose squared masses at tree level are $m_{H^\pm}^2 = m_{A^0}^2 + m_{\rm W}^2$. The charged Goldstone bosons and neutral Goldstone bosons are denoted respectively

$$\begin{aligned} &G^\pm = \cos\beta H_d^\pm + \sin\beta H_u^\pm, \qquad G^0 = \cos\beta P_d^0 + \sin\beta P_u^0 \ , \\ &G_B^0 = \cos\beta_B P_B^0 + \sin\beta_B \overline{P}_B^0, \quad G_L^0 = \cos\beta_L P_L^0 + \sin\beta_L \overline{P}_L^0, \end{aligned} \tag{7}$$

with $\tan\beta = \upsilon_u/\upsilon_d$, $\tan\beta_B = \overline{\upsilon}_B/\upsilon_B$, $\tan\beta_L = \overline{\upsilon}_L/\upsilon_L$.

$$\begin{aligned} &A^0 = -\sin\beta P_d^0 + \cos\beta P_u^0, \quad A_B^0 = -\sin\beta_B P_B^0 + \cos\beta_B \overline{P}_B^0 \ , \\ &A_L^0 = -\sin\beta_L P_L^0 + \cos\beta_L \overline{P}_L^0, \end{aligned} \tag{8}$$

are the physical neutral pseudoscalar fields, and their masses at tree level read as[15]

$$m_{A^0}^2 = \frac{B\mu_H}{\cos\beta\sin\beta}, \quad m_{A_B^0}^2 = \frac{B_B\mu_B}{\cos\beta_B\sin\beta_B}, \quad m_{A_L^0}^2 = \frac{B_L\mu_L}{\cos\beta_L\sin\beta_L}. \tag{9}$$

The lightest neutral CP-even Higgs h^0 is obtained from diagonalizing the mass squared matrix of neutral CP-even Higgs in the sector (H_d^0,H_u^0)

$$\begin{aligned} &\begin{pmatrix} H^0 \\ h^0 \end{pmatrix} = \begin{pmatrix} \cos\alpha & \sin\alpha \\ -\sin\alpha & \cos\alpha \end{pmatrix} \begin{pmatrix} H_d^0 \\ H_u^0 \end{pmatrix}, \\ &\tan 2\alpha = \frac{m_Z^2 + m_{A^0}^2}{m_Z^2 - m_{A^0}^2} \tan 2\beta \ . \end{aligned} \tag{10}$$

Φ_B^0 and φ_B^0 mix together and the mass squared matrix is

$$\mathcal{M}_{EB}^2 = \begin{pmatrix} m_{Z_B}^2 \cos^2\beta_B + m_{A_B^0}^2 \sin^2\beta_B, & (m_{Z_B}^2 + m_{A_B^0}^2)\cos\beta_B\sin\beta_B \\ (m_{Z_B}^2 + m_{A_B^0}^2)\cos\beta_B\sin\beta_B, & m_{Z_B}^2\sin^2\beta_B + m_{A_B^0}^2\cos^2\beta_B \end{pmatrix} , \tag{11}$$

with $v_{B_t} = \sqrt{v_{_B}^2 + \overline{v}_{_B}^2}$. $m_{_{Z_B}} = g_{_B} v_{B_t}$ denotes the mass of neutral $U(1)_{_B}$ gauge boson $Z_{_B}$. Two mass eigenstates can be gotten

$$\begin{pmatrix} H_{_B}^0 \\ h_{_B}^0 \end{pmatrix} = \begin{pmatrix} \cos\alpha_{_B} & \sin\alpha_{_B} \\ -\sin\alpha_{_B} & \cos\alpha_{_B} \end{pmatrix} \begin{pmatrix} \Phi_{_B}^0 \\ \varphi_{_B}^0 \end{pmatrix} , \tag{12}$$

by the mixing angle $\alpha_{_B}$ that is defined as

$$\tan 2\alpha_{_B} = \frac{m_{_{Z_B}}^2 + m_{_{A_B^0}}^2}{m_{_{Z_B}}^2 - m_{_{A_B^0}}^2} \tan 2\beta_{_B}. \tag{13}$$

In the same way, we obtain the mass squared matrix for $(\Phi_{_L}^0,\ \varphi_{_L}^0)$

$$\mathcal{M}_{_{EL}}^2 = \begin{pmatrix} m_{_{Z_L}}^2 \cos^2\beta_{_L} + m_{_{A_L^0}}^2 \sin^2\beta_{_L}, & (m_{_{Z_L}}^2 + m_{_{A_L^0}}^2)\cos\beta_{_L}\sin\beta_{_L} \\ (m_{_{Z_L}}^2 + m_{_{A_L^0}}^2)\cos\beta_{_L}\sin\beta_{_L}, & m_{_{Z_L}}^2 \sin^2\beta_{_L} + m_{_{A_L^0}}^2 \cos^2\beta_{_L} \end{pmatrix}, \tag{14}$$

with $v_{L_t} = \sqrt{v_{_L}^2 + \overline{v}_{_L}^2}$. $m_{_{Z_L}} = 2g_{_L} v_{L_t}$ represents the mass of neutral $U(1)_{_L}$ gauge boson $Z_{_L}$. In BLMSSM, the authors[15, 20] analyze the mass matrices of exotic quarks, exotic squarks and some exotic sleptons.

With the introduced superfields $\hat{N}^c$, three neutrinos obtain tiny masses through the see-saw mechanism. After symmetry breaking, we obtain the mass matrix for neutrinos in the basis (ν, N^c)[21]

$$\begin{pmatrix} 0 & \frac{v_u}{\sqrt{2}}(Y_\nu)^{IJ} \\ \frac{v_u}{\sqrt{2}}(Y_\nu^T)^{IJ} & \frac{\bar{v}_L}{\sqrt{2}}(\lambda_{N^c})^{IJ} \end{pmatrix}. \tag{15}$$

Eq.(15) can be diagonalized by the unitary matrix U_ν. Then, one gets three light and three heavy neutrino mass eigenstates.

The new gaugino λ_L and the superpartners of the $SU(2)_L$ singlets Φ_L, φ_L mix, which produce three lepton neutralinos in the base $(i\lambda_L, \psi_{\Phi_L}, \psi_{\varphi_L})$[17].

$$\mathcal{L}_{\chi_L^0} = \frac{1}{2}(i\lambda_L, \psi_{\Phi_L}, \psi_{\varphi_L}) \begin{pmatrix} 2M_L & 2v_L g_L & -2\bar{v}_L g_L \\ 2v_L g_L & 0 & -\mu_L \\ -2\bar{v}_L g_L & -\mu_L & 0 \end{pmatrix} \begin{pmatrix} i\lambda_L \\ \psi_{\Phi_L} \\ \psi_{\varphi_L} \end{pmatrix} + h.c. \tag{16}$$

Using Z_{N_L}, one can diagonalize the mass matrix in Eq.(16) to obtain three lepton neutralino masses.

In BLMSSM, the mass squared matrix of slepton is different from that in MSSM, because of the contributions from Eqs.(2,3). The corrected mass squared matrix of slepton reads as

$$\begin{pmatrix} (\mathcal{M}_L^2)_{LL} & (\mathcal{M}_L^2)_{LR} \\ (\mathcal{M}_L^2)_{LR}^\dagger & (\mathcal{M}_L^2)_{RR} \end{pmatrix}. \tag{17}$$

$(\mathcal{M}_L^2)_{LL}$, $(\mathcal{M}_L^2)_{LR}$ and $(\mathcal{M}_L^2)_{RR}$ are shown here

$$\begin{aligned} (\mathcal{M}_L^2)_{LL} &= \frac{(g_1^2-g_2^2)(v_d^2-v_u^2)}{8}\delta_{IJ} + g_L^2(\bar{v}_L^2 - v_L^2)\delta_{IJ} + m_{l^I}^2\delta_{IJ} + (m_{\tilde{L}}^2)_{IJ}, \\ (\mathcal{M}_L^2)_{LR} &= \frac{\mu^* v_u}{\sqrt{2}}(Y_l)_{IJ} - \frac{v_u}{\sqrt{2}}(A_l')_{IJ} + \frac{v_d}{\sqrt{2}}(A_l)_{IJ}, \\ (\mathcal{M}_L^2)_{RR} &= \frac{g_1^2(v_u^2-v_d^2)}{4}\delta_{IJ} - g_L^2(\bar{v}_L^2 - v_L^2)\delta_{IJ} + m_{l^I}^2\delta_{IJ} + (m_{\tilde{R}}^2)_{IJ}. \end{aligned} \tag{18}$$

The unitary matrix $Z_{\tilde{L}}$ is used to rotate slepton mass squared matrix to mass eigenstates.

There are six sneutrinos, whose mass squared matrix is deduced from the superpotential and the soft breaking terms in Eqs.(2,3). In the base $\tilde{n}^T = (\tilde{\nu}, \tilde{N}^c)$, the concrete forms for the sneutrino mass squared matrix $\mathcal{M}_{\tilde{n}}$ are shown here

$$\begin{aligned} \mathcal{M}_{\tilde{n}}^2(\tilde{\nu}_I^*\tilde{\nu}_J) &= \frac{g_1^2+g_2^2}{8}(v_d^2-v_u^2)\delta_{IJ} + g_L^2(\overline{v}_L^2 - v_L^2)\delta_{IJ} + \frac{v_u^2}{2}(Y_\nu^\dagger Y_\nu)_{IJ} + (m_{\tilde{L}}^2)_{IJ}, \\ \mathcal{M}_{\tilde{n}}^2(\tilde{N}_I^{c*}\tilde{N}_J^c) &= -g_L^2(\overline{v}_L^2 - v_L^2)\delta_{IJ} + \frac{v_u^2}{2}(Y_\nu^\dagger Y_\nu)_{IJ} + 2\overline{v}_L^2(\lambda_{N^c}^\dagger \lambda_{N^c})_{IJ} \\ &\quad +(m_{\tilde{N}^c}^2)_{IJ} + \mu_L\frac{v_L}{\sqrt{2}}(\lambda_{N^c})_{IJ} - \frac{\overline{v}_L}{\sqrt{2}}(A_{N^c})_{IJ}(\lambda_{N^c})_{IJ}, \\ \mathcal{M}_{\tilde{n}}^2(\tilde{\nu}_I\tilde{N}_J^c) &= \mu^*\frac{v_d}{\sqrt{2}}(Y_\nu)_{IJ} - v_u\overline{v}_L(Y_\nu^\dagger\lambda_{N^c})_{IJ} + \frac{v_u}{\sqrt{2}}(A_N)_{IJ}(Y_\nu)_{IJ}. \end{aligned} \tag{19}$$

The superfields $\tilde{N}^c$ in BLMSSM lead to the corrections for the couplings existed in MSSM and some corrected couplings are deduced. We give out the couplings for W-lepton-neutrino and Z-neutrino-neutrino

$$\begin{aligned} \mathcal{L}_{WL\nu} &= -\frac{e}{\sqrt{2}s_W}W_\mu^+\sum_{I,J=1}^{3}\sum_{i=1}^{2}(U_{\nu^{IJ}}^\dagger)^{i1}\bar{\nu}_i^I\gamma^\mu P_L e^J, \\ \mathcal{L}_{Z\nu\nu} &= -\frac{e}{2s_W c_W}Z_\mu\sum_{I,J,K=1}^{3}\sum_{i,j=1}^{2}(U_{\nu^{IK}}^\dagger)^{i1}U_{\nu^{JK}}^{1j}\bar{\nu}_i^I\gamma^\mu P_L\nu_j^J. \end{aligned} \tag{20}$$

The charged Higgs-lepton-neutrino couplings are

$$\begin{aligned} \mathcal{L}_{H^\pm L\nu} &= \sum_{I,J=1}^{3}\sum_{i=1}^{2}G^\pm\bar{e}^J\Big(Y_l^{IJ}\cos\beta U_{\nu^{IJ}}^{1i}P_L - Y_\nu^{IJ*}\sin\beta U_{\nu^{IJ}}^{2i}P_R\Big)\nu_i^I \\ &- \sum_{I,J=1}^{3}\sum_{i=1}^{2}H^\pm\bar{e}^J\Big(Y_l^{IJ}\sin\beta U_{\nu^{IJ}}^{1i}P_L + Y_\nu^{IJ*}\cos\beta U_{\nu^{IJ}}^{2i}P_R\Big)\nu_i^I + h.c. \end{aligned} \tag{21}$$

The corrected chargino-lepton-sneutrino couplings read as

$$\begin{aligned}\mathcal{L}_{\chi^{\pm}L\tilde{\nu}} = &- \sum_{I,J=1}^{3}\sum_{i,j=1}^{2} \bar{\chi}_j^{-}\Big(Y_l^{IJ} Z_-^{2j*}(Z^{\dagger}_{\nu^{IJ}})^{i1} P_R \\ &+[\frac{e}{s_W} Z_+^{1j}(Z^{\dagger}_{\nu^{IJ}})^{i1} + Y_{\nu}^{IJ} Z_+^{2j}(Z^{\dagger}_{\nu^{IJ}})^{i2}] P_L\Big) e^J \tilde{\nu}_i^{I*}. \end{aligned} \qquad (22)$$

We also obtain the adapted Z-sneutrino-sneutrino couplings as follows

$$\mathcal{L}_{Z\tilde{\nu}\tilde{\nu}} = -\frac{e}{2s_W c_W} Z_{\mu} \sum_{I,J,K=1}^{3}\sum_{i,j=1}^{2} (Z^{\dagger}_{\nu^{IK}})^{i1} Z^{1j}_{\nu^{JK}} \tilde{\nu}_i^{I*} \mathtt{i}(\overrightarrow{\partial}^{\mu} - \overleftarrow{\partial}^{\mu}) \tilde{\nu}_j^{J}. \qquad (23)$$

In BLMSSM, there are new couplings that are deduced from the interactions of gauge and matter multiplets $ig\sqrt{2}T^a_{ij}(\lambda^a\psi_j A_i^* - \bar{\lambda}^a\bar{\psi}_i A_j)$. After calculation, the lepton-slepton-lepton neutralino couplings are obtained

$$\mathcal{L}_{l\chi_L^0\tilde{L}} = \sqrt{2} g_L \bar{\chi}^0_{L_j}\Big(Z^{1j}_{N_L} Z_L^{Ii} P_L - Z^{1j*}_{N_L} Z_L^{(I+3)i} P_R\Big) l^I \tilde{L}_i^{+} + h.c. \qquad (24)$$

III. CHARGED LEPTON FLAVOR VIOLATION IN THE BLMSSM

In this section, the CLFV processes $l_j \to l_i + \gamma$ and $l_j \to 3l_i$ are studied in the BLMSSM. For convenience, the triangle, penguin and box diagrams are analyzed in the generic form, which can simplify the work.

A. Rare decays $l_j \to l_i + \gamma$

When the external leptons are all on shell, we can generally write the amplitudes for $l_j \to l_i + \gamma$ as

$$\begin{aligned}\mathcal{M} = e\epsilon^{\mu}\bar{u}_i(p+q)\Big[&q^2\gamma_{\mu}(C_1^L P_L + C_1^R P_R) \\ &+ m_{l_j} i\sigma_{\mu\nu}q^{\nu}(C_2^L P_L + C_2^R P_R)\Big]u_j(p)\ , \end{aligned} \qquad (25)$$

where p is the injecting lepton momentum, q is the photon momentum, and m_{l_j} is the mass of the j-th generation charged lepton. $u_i(p)$ and $v_i(p)$ are the wave functions for the external leptons. The relevant Feynman diagrams are shown in Fig.1. The final Wilson coefficients $C_1^L, C_1^R, C_2^L, C_2^R$ are obtained from the sum of these diagrams' amplitudes.

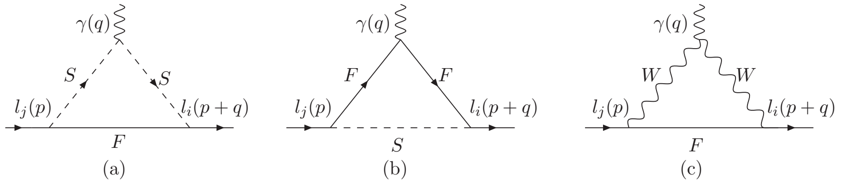

FIG. 1: The one loop diagrams for $l_j \to l_i + \gamma$, with F representing Dirac(Majorana) particles.

The contributions from the virtual neutral fermion diagrams Fig.1(a) are denoted by $C_\alpha^{L,R}(n), \alpha = 1, 2$. We give out the deduced results in the following form,

$$\begin{aligned}
C_1^L(n) &= \sum_{F=\chi^0,\chi_L^0,\nu}\;\sum_{S=\tilde{L},\tilde{L},H^\pm} \frac{1}{6m_W^2} H_R^{SF\bar{l}_i} H_L^{S^* l_j \bar{F}} I_1(x_F, x_S)\ , \\
C_2^L(n) &= \sum_{F=\chi^0,\chi_L^0,\nu}\;\sum_{S=\tilde{L},\tilde{L},H^\pm} \frac{m_F}{m_{l_j} m_W^2} H_L^{SF\bar{l}_i} H_L^{S^* l_j \bar{F}} \Big[I_2(x_F, x_S) - I_3(x_F, x_S)\Big]\ , \\
C_\alpha^R(n) &= C_\alpha^L(n)\Big|_{L\leftrightarrow R}, \quad \alpha = 1, 2,
\end{aligned} \tag{26}$$

with $x = m^2/m_W^2$ and m representing the mass for the corresponding particle. $H_{L,R}^{SF\bar{l}_i}$ and $H_{L,R}^{S^* l_j \bar{F}}$ are the corresponding couplings of the left(right)-hand parts in the Lagrangian. The one-loop functions $I_i(x_1, x_2), i = 1 \ldots 3$ are collected here

$$\begin{aligned}
I_1(x_1, x_2) &= \frac{1}{96\pi^2}\Big[\frac{11 + 6\ln x_2}{(x_2 - x_1)} - \frac{15x_2 + 18x_2 \ln x_2}{(x_2 - x_1)^2} + \frac{6x_2^2 + 18x_2^2 \ln x_2}{(x_2 - x_1)^3}, \\
&\quad + \frac{6x_1^3 \ln x_1 - 6x_2^3 \ln x_2}{(x_2 - x_1)^4}\Big]\ .
\end{aligned} \tag{27}$$

$$I_2(x_1, x_2) = \frac{1}{32\pi^2}\Big[\frac{3 + 2\ln x_2}{(x_2 - x_1)} - \frac{2x_2 + 4x_2 \ln x_2}{(x_2 - x_1)^2} - \frac{2x_1^2 \ln x_1}{(x_2 - x_1)^3} + \frac{2x_2^2 \ln x_2}{(x_2 - x_1)^3}\Big]\ , \tag{28}$$

$$I_3(x_1, x_2) = \frac{1}{16\pi^2}\Big[\frac{1 + \ln x_2}{(x_2 - x_1)} + \frac{x_1 \ln x_1 - x_2 \ln x_2}{(x_2 - x_1)^2}\Big]\ . \tag{29}$$

$C_\alpha^{L,R}(c), \alpha = 1, 2$ stand for the coefficients from the virtual charged fermion diagrams Fig.1(b), and they are shown here

$$\begin{aligned}
C_1^L(c) &= \sum_{F=\chi^\pm}\sum_{S=\tilde{\nu}} \frac{1}{6m_W^2} H_R^{SF\bar{l}_i} H_L^{S^* l_j \bar{F}} \Big[I_3(x_F, x_S) - 2I_4(x_F, x_S) - I_1(x_F, x_S)\Big]\ , \\
C_2^L(c) &= \sum_{F=\chi^\pm}\sum_{S=\tilde{\nu}} \frac{m_F}{m_{l_j} m_W^2} H_L^{SF\bar{l}_i} H_L^{S^* l_j \bar{F}} \Big[I_3(x_F, x_S) - I_4(x_F, x_S) - I_1(x_F, x_S)\Big]\ , \\
C_\alpha^R(c) &= C_\alpha^L(c)\Big|_{L\leftrightarrow R}, \quad \alpha = 1, 2.
\end{aligned} \tag{30}$$

with

$$I_4(x_1, x_2) = \frac{1}{16\pi^2}\Big[-\frac{1 + \ln x_1}{(x_2 - x_1)} - \frac{x_1 \ln x_1 - x_2 \ln x_2}{(x_2 - x_1)^2}\Big]\ . \tag{31}$$

Because three light neutrinos and three heavy neutrinos mix together, the virtual W diagrams Fig.1(c) have corrections to the CLFV process $l_j \to l_i\gamma$. The corresponding coefficients are denoted by $C_\alpha^{L,R}(W)(\alpha = 1, 2)$

$$\begin{aligned}
&C_1^L(W) = \sum_{F=\nu} \frac{-1}{2m_W^2} H_L^{WF\bar{l}_i} H_L^{W^* l_j \bar{F}} \Big[I_2(x_F, x_W) + I_1(x_F, x_W)\Big],\\
&C_2^L(W) = \sum_{F=\nu} \frac{1}{m_W^2} H_L^{WF\bar{l}_i} H_L^{W^* l_j \bar{F}} (1 + \frac{m_{l_i}}{m_{l_j}}) \Big[2I_2(x_F, x_W) - \frac{1}{3} I_1(x_F, x_W)\Big],\\
&C_\alpha^R(W) = 0, \quad \alpha = 1, 2. \qquad (32)
\end{aligned}$$

The total coefficients are the sum of Eqs.(26)(30)(32)

$$C_\alpha^{L,R} = C_\alpha^{L,R}(n) + C_\alpha^{L,R}(c) + C_\alpha^{L,R}(W), \quad i = 1, 2. \qquad (33)$$

With the Eq.(25), the decay width for $l_j \to l_i + \gamma$ can be expressed as[9]

$$\Gamma(l_j \to l_i + \gamma) = \frac{e^2}{16\pi} m_{l_j}^5 \left(\left|C_2^L\right|^2 + \left|C_2^R\right|^2\right). \qquad (34)$$

B. Rare decays $l_j \to 3l_i$

The CLFV processes $l_j \to 3l_i$ are very interesting. Both penguin-type diagrams and box-type diagrams have contributions to the effective Lagrangian. With Eq.(25), one can obtain the γ-penguin contributions in the following form,

$$\begin{aligned}
T_{\gamma-\mathrm{p}} = &\bar{u}_i(p_1)\Big[q^2\gamma_\mu(C_1^L P_L + C_1^R P_R) + m_{l_j} i\sigma_{\mu\nu} q^\nu (C_2^L P_L + C_2^R P_R)\Big] u_j(p)\\
&\times \frac{e^2}{q^2} \bar{u}_i(p_2)\gamma^\mu v_i(p_3) - (p_1 \leftrightarrow p_2). \qquad (35)
\end{aligned}$$

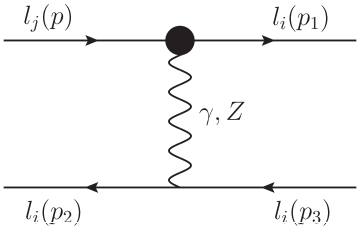

FIG. 2: The penguin-type diagrams for CLFV process $l_j \to 3l_i$.

The contributions from Z-penguin diagrams are depicted by the Fig.2, and deduced in the same way as γ-penguin diagrams,

$$T_{Z-\mathrm{p}} = \frac{e^2}{m_Z^2} \bar{u}_i(p_1)\gamma_\mu(N_L P_L + N_R P_R) u_j(p) \bar{u}_i(p_2)\gamma^\mu \Big(H_L^{Z l_i \bar{l}_i} P_L$$

$$
\begin{aligned}
&\quad + H_R^{Zl_i\bar{l}_i} P_R\Big) v_i(p_3) - (p_1 \leftrightarrow p_2)\ , \\
&N_{L,R} = N_{L,R}(S) + N_{L,R}(W)\ .
\end{aligned}
\tag{36}
$$

The concrete forms of the effective couplings $N_L(S),\ N_R(S)$ read as

$$
\begin{aligned}
N_L(S) = &\frac{1}{2e^2} \sum_{F=\chi^0,\chi^\pm,\nu} \sum_{S=\tilde{L},\tilde{\nu},H^\pm} \Big[\frac{2m_{F_1}m_{F_2}}{m_W^2} H_R^{SF_2\bar{l}_i} H_L^{ZF_1\bar{F}_2} H_L^{S^*l_j\bar{F}_1} G_1(x_S, x_{F_2}, x_{F_1}) \\
&+ H_R^{S_2F\bar{l}_i} H_R^{ZS_1S_2^*} H_L^{S_1^*l_j\bar{F}} G_2(x_F, x_{S_1}, x_{S_2}) - H_R^{SF_2\bar{l}_i} H_R^{ZF_1\bar{F}_2} H_L^{S^*l_j\bar{F}_1} G_2(x_S, x_{F_2}, x_{F_1})\Big] \\
&+ \sum_{F=\chi_L^0} \sum_{S=\tilde{L}} \Big[H_R^{S_2F\bar{l}_i} H_R^{ZS_1S_2^*} H_L^{S_1^*l_j\bar{F}} G_2(x_F, x_{S_1}, x_{S_2})\Big], \\
N_R(S) = &\ N_L(S)\big|_{\,L\leftrightarrow R}\ .
\end{aligned}
\tag{37}
$$

The functions $G_1(x_1, x_2, x_3)$ and $G_2(x_1, x_2, x_3)$ are

$$
\begin{aligned}
G_1(x_1, x_2, x_3) = &\frac{1}{16\pi^2}\Big[\frac{x_1 \ln x_1}{(x_1 - x_2)(x_1 - x_3)} + \frac{x_2 \ln x_2}{(x_2 - x_1)(x_2 - x_3)} \\
&+ \frac{x_3 \ln x_3}{(x_3 - x_1)(x_3 - x_2)}\Big],
\end{aligned}
\tag{38}
$$

$$
\begin{aligned}
G_2(x_1, x_2, x_3) = &\frac{1}{16\pi^2}\Big[- (\Delta + 1 + \ln x_\mu) + \frac{x_1^2 \ln x_1}{(x_1 - x_2)(x_1 - x_3)} \\
&+ \frac{x_2^2 \ln x_2}{(x_2 - x_1)(x_2 - x_3)} + \frac{x_3^2 \ln x_3}{(x_3 - x_1)(x_3 - x_2)}\Big].
\end{aligned}
\tag{39}
$$

$G_2(x_1, x_2, x_3)$ has infinite term, and to obtain finite results we use $\overline{MS}$ subtraction and $\overline{DR}$ scheme.

We deduce the effective couplings $N_{L,R}(W)$ in detail and keep the small m_i terms.

$$
\begin{aligned}
N_L(W) = &\frac{c_W}{e s_W} \sum_{F=\nu} H_L^{WF\bar{l}_i} H_L^{W^*l_j\bar{F}} \Big[G_3(x_F, x_W) + 2(x_i + x_j)[I_1(x_F, x_W) - I_2(x_F, x_W)]\Big] \\
&+ \frac{1}{e^2} \sum_{F_1,F_2=\nu} H_L^{WF_2\bar{l}_i} H_L^{W^*l_j\bar{F}_1} H_L^{Z^*F_1\bar{F}_2} \Big(- \frac{3}{32\pi^2} - G_2(x_W, x_{F_1}, x_{F_2}) \\
&+ x_j[\frac{1}{3} G_4(x_W, x_{F_1}, x_{F_2}) + G_5(x_W, x_{F_1}, x_{F_2})]\Big), \\
N_R(W) = &\frac{c_W}{e s_W} \sum_{F=\nu} H_L^{WF\bar{l}_i} H_L^{W^*l_j\bar{F}} \Big[2\sqrt{x_i x_j}[I_1(x_F, x_W) - I_2(x_F, x_W)]\Big] \\
&+ \frac{1}{e^2} \sum_{F_1,F_2=\nu} H_L^{WF_2\bar{l}_i} H_L^{W^*l_j\bar{F}_1} H_L^{Z^*F_1\bar{F}_2} \sqrt{x_i x_j} \Big(2G_1(x_W, x_{F_1}, x_{F_2}) \\
&- \frac{1}{3} G_4(x_W, x_{F_1}, x_{F_2}) - 2G_5(x_W, x_{F_1}, x_{F_2})\Big).
\end{aligned}
\tag{40}
$$

The concrete expressions for the functions $G_3(x_1, x_2), G_4(x_1, x_2, x_3)$ and $G_5(x_1, x_2, x_3)$ are collected here

$$
G_3(x_1, x_2) = \frac{-1}{16\pi^2}\Big((\Delta + \ln x_\mu + 1) + \frac{x_2^2 \ln x_2 - x_1^2 \ln x_1}{(x_2 - x_1)^2} + \frac{x_2 + 2x_2 \ln x_2}{x_1 - x_2} - \frac{1}{2}\Big),
$$

$$
\begin{aligned}
G_4(x_1,x_2,x_3) &= \frac{1}{32\pi^2}\Big(\frac{2x_1^3[3x_1(x_1-x_2-x_3)+x_2^2+x_2x_3+x_3^2]\ln x_1}{(x_1-x_2)^3(x_1-x_3)^3} \\
&\quad -\frac{2(3x_1^2-3x_1x_2+x_2^2)x_2\ln x_2}{(x_1-x_2)^3(x_2-x_3)}+\frac{2(3x_1^2-3x_1x_3+x_3^2)x_3\ln x_3}{(x_1-x_3)^3(x_2-x_3)} \\
&\quad -\frac{x_1[5x_1^2-3x_1(x_2+x_3)+x_2x_3]}{(x_1-x_2)^2(x_1-x_3)^2}\Big), \\
G_5(x_1,x_2,x_3) &= \frac{1}{16\pi^2}\Big(\frac{x_1^2(2x_1-x_2-x_3)\ln x_1}{(x_1-x_2)^2(x_1-x_3)^2}+\frac{x_2(x_2-2x_1)\ln x_2}{(x_1-x_2)^2(x_2-x_3)} \\
&\quad -\frac{x_1}{(x_1-x_2)(x_1-x_3)}+\frac{x_3(2x_1-x_3)\ln x_3}{(x_1-x_3)^2(x_2-x_3)}\Big). \qquad (41)
\end{aligned}
$$

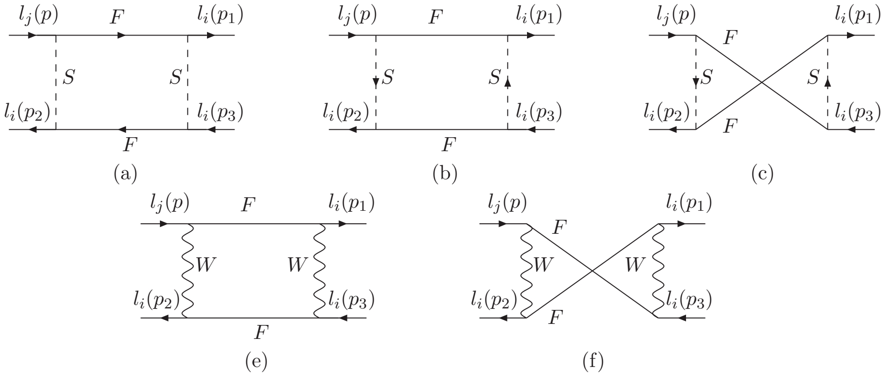

FIG. 3: The box-type diagrams for CLFV processes $l_j \to 3l_i$ with F representing Dirac(Majorana) particles.

The box-type diagrams drawn in Fig.3 can be written as

$$\begin{aligned}
T_{box} = & \Big\{B_1^L e^2 \bar{u}_i(p_1)\gamma_\mu P_L u_j(p)\bar{u}_i(p_2)\gamma^\mu P_L v_i(p_3) + (L \leftrightarrow R)\Big\} \\
& + \Big\{B_2^L e^2 \Big[\bar{u}_i(p_1)\gamma_\mu P_L u_j(p)\bar{u}_i(p_2)\gamma^\mu P_R v_i(p_3) - (p_1 \leftrightarrow p_2)\Big] + (L \leftrightarrow R)\Big\} \\
& + \Big\{B_3^L e^2 \Big[\bar{u}_i(p_1) P_L u_j(p)\bar{u}_i(p_2) P_L v_i(p_3) - (p_1 \leftrightarrow p_2)\Big] + (L \leftrightarrow R)\Big\} \\
& + \Big\{B_4^L e^2 \Big[\bar{u}_i(p_1)\sigma_{\mu\nu} P_L u_j(p)\bar{u}_i(p_2)\sigma^{\mu\nu} P_L v_i(p_3) - (p_1 \leftrightarrow p_2)\Big] + (L \leftrightarrow R)\Big\} \\
& + \Big\{B_5^L e^2 \Big[\bar{u}_i(p_1) P_L u_j(p)\bar{u}_i(p_2) P_R v_i(p_3) - (p_1 \leftrightarrow p_2)\Big] + (L \leftrightarrow R)\Big\}. \qquad (42)
\end{aligned}$$

From the box-type diagrams, we obtain the virtual chargino contributions to the effective couplings $B_\beta^{L,R}(c)$ with $\beta = 1\ldots5$

$$\begin{aligned}
B_1^L(c) = & \sum_{F_1,F_2=\chi^\pm}\sum_{S_1,S_2=\tilde{\nu}} \frac{1}{2e^2 m_W^2} G_6(x_{F_1},x_{F_2},x_{S_1},x_{S_2}) H_R^{S_2 F_1 \bar{l}_i} H_L^{S_1 l_j \bar{F}_1} H_R^{S_1 F_2 \bar{l}_i} H_L^{S_2 l_i \bar{F}_2}, \\
B_2^L(c) = & \sum_{F_1,F_2=\chi^\pm}\sum_{S_1,S_2=\tilde{\nu}} \Big[\frac{1}{4e^2 m_W^2} G_6(x_{F_1},x_{F_2},x_{S_1},x_{S_2}) H_R^{S_2 F_1 \bar{l}_i} H_L^{S_1 l_j \bar{F}_1} H_L^{S_1 F_2 \bar{l}_i} H_R^{S_2 l_i \bar{F}_2} \\
& - \frac{m_{F_1} m_{F_2}}{2e^2 m_W^4} G_7(x_{F_1},x_{F_2},x_{S_1},x_{S_2}) H_R^{S_2 F_1 \bar{l}_i} H_R^{S_1 l_j \bar{F}_1} H_L^{S_1 F_2 \bar{l}_i} H_L^{S_2 l_i \bar{F}_2}\Big], \\
B_3^L(c) = & \sum_{F_1,F_2=\chi^\pm}\sum_{S_1,S_2=\tilde{\nu}} \frac{m_{F_1} m_{F_2}}{e^2 m_W^4} G_7(x_{F_1},x_{F_2},x_{S_1},x_{S_2}) H_L^{S_2 F_1 \bar{l}_i} H_L^{S_1 l_j \bar{F}_1} H_L^{S_1 F_2 \bar{l}_i} H_L^{S_2 l_i \bar{F}_2}, \\
B_4^L(c) = & B_5^L(c) = 0\,, \quad B_\beta^R(c) = B_\beta^L(c)\Big|_{L\leftrightarrow R}, \quad \beta = 1\ldots5. \qquad (43)
\end{aligned}$$

with

$$\begin{aligned}
G_6(x_1,x_2,x_3,x_4) = & \frac{1}{16\pi^2}\Big[\frac{x_1^2 \ln x_1}{(x_1-x_2)(x_1-x_3)(x_1-x_4)} + \frac{x_2^2 \ln x_2}{(x_2-x_1)(x_2-x_3)(x_2-x_4)} \\
& + \frac{x_3^2 \ln x_3}{(x_3-x_1)(x_3-x_2)(x_3-x_4)} + \frac{x_4^2 \ln x_4}{(x_4-x_1)(x_4-x_2)(x_4-x_3)}\Big]\,,
\end{aligned}$$

$$\begin{aligned}G_7(x_1,x_2,x_3,x_4) = &\frac{1}{16\pi^2}\Big[\frac{x_1\ln x_1}{(x_1-x_2)(x_1-x_3)(x_1-x_4)} + \frac{x_2\ln x_2}{(x_2-x_1)(x_2-x_3)(x_2-x_4)} \\ &+\frac{x_3\ln x_3}{(x_3-x_1)(x_3-x_2)(x_3-x_4)} + \frac{x_4\ln x_4}{(x_4-x_1)(x_4-x_2)(x_4-x_3)}\Big]. \end{aligned} \tag{44}$$

For the box-type diagrams, the neutralino-slepton, neutrino-charged Higgs and lepton neutralino-slepton contributions to the effective couplings $B_\beta^{L,R}(n)$ are gotten,

$$\begin{aligned}
B_1^L(n) = &\sum_{F_1,F_2=\chi^0,\chi_L^0,\nu}\ \sum_{S_1,S_2=\tilde{L},\tilde{L},H^\pm} \frac{m_{F_1}m_{F_2}}{e^2m_W^4}G_7(x_{F_1},x_{F_2},x_{S_1},x_{S_2})H_L^{S_2F_1\bar{l}_i}H_L^{S_1^*l_j\bar{F}_1}H_R^{S_2F_2\bar{l}_i}H_R^{S_1^*l_i\bar{F}_2} \\
&+\frac{1}{2e^2m_W^2}G_6(x_{F_1},x_{F_2},x_{S_1},x_{S_2})\Big[H_R^{S_2F_1\bar{l}_i}H_L^{S_1^*l_j\bar{F}_1}H_R^{S_1F_2\bar{l}_i}H_L^{S_2^*l_i\bar{F}_2} \\
&+H_L^{S_2F_1\bar{l}_i}H_R^{S_1^*l_j\bar{F}_1}H_R^{S_2F_2\bar{l}_i}H_L^{S_1^*l_i\bar{F}_2}\Big], \\
B_2^L(n) = &\sum_{F_1,F_2=\chi^0,\chi_L^0,\nu}\ \sum_{S_1,S_2=\tilde{L},\tilde{L},H^\pm} -\frac{m_{F_1}m_{F_2}}{2e^2m_W^4}G_7(x_{F_1},x_{F_2},x_{S_1},x_{S_2})H_R^{S_2F_1\bar{l}_i}H_R^{S_1^*l_j\bar{F}_1}H_L^{S_1F_2\bar{l}_i}H_L^{S_2^*l_i\bar{F}_2} \\
&+\frac{1}{4e^2m_W^2}G_6(x_{F_1},x_{F_2},x_{S_1},x_{S_2})\Big[H_R^{S_2F_1\bar{l}_i}H_L^{S_1^*l_j\bar{F}_1}H_L^{S_1F_2\bar{l}_i}H_R^{S_2^*l_i\bar{F}_2} \\
&+H_R^{S_2F_1\bar{l}_i}H_L^{S_1^*l_j\bar{F}_1}H_R^{S_2F_2\bar{l}_i}H_L^{S_1^*l_i\bar{F}_2}\Big], \\
B_3^L(n) = &\sum_{F_1,F_2=\chi^0,\chi_L^0,\nu}\ \sum_{S_1,S_2=\tilde{L},\tilde{L},H^\pm} \frac{m_{F_1}m_{F_2}}{e^2m_W^4}G_7(x_{F_1},x_{F_2},x_{S_1},x_{S_2})\Big[H_L^{S_2F_1\bar{l}_i}H_L^{S_1^*l_j\bar{F}_1}H_L^{S_1F_2\bar{l}_i}H_L^{S_2^*l_i\bar{F}_2} \\
&-\frac{1}{2}\,H_L^{S_2F_1\bar{l}_i}H_L^{S_1^*l_j\bar{F}_1}H_L^{S_2F_2\bar{l}_i}H_L^{S_1^*l_i\bar{F}_2}\Big], \\
B_4^L(n) = &\sum_{F_1,F_2=\chi^0,\chi_L^0,\nu}\ \sum_{S_1,S_2=\tilde{L},\tilde{L},H^\pm} \frac{m_{F_1}m_{F_2}}{8e^2m_W^4}G_7(x_{F_1},x_{F_2},x_{S_1},x_{S_2})H_L^{S_2F_1\bar{l}_i}H_L^{S_1^*l_j\bar{F}_1}H_L^{S_2F_2\bar{l}_i}H_L^{S_1^*l_i\bar{F}_2}, \\
B_5^L(n) = &\,0, \qquad B_\beta^R(n) = B_\beta^L(n)\Big|_{L\leftrightarrow R}, \qquad \beta = 1\ldots 5.
\end{aligned} \tag{45}$$

We also deduce the box-type contributions from virtual W-neutrino

$$\begin{aligned}
B_1^L(W) = &\sum_{F_1,F_2=\nu}\frac{1}{e^2m_W^2}\Big[-\frac{\partial}{\partial x_W}G_2(x_W,x_{F_1},x_{F_2})H_L^{Wl_j\bar{F}_1}H_L^{W^*F_1\bar{l}_i}H_L^{W^*F_2\bar{l}_i}H_L^{Wl_i\bar{F}_2} \\
&-2\frac{m_{F_1}m_{F_2}}{m_W^2}\frac{\partial}{\partial x_W}G_1(x_W,x_{F_1},x_{F_2})H_L^{Wl_j\bar{F}_1}H_L^{W^*F_2\bar{l}_i}H_L^{Wl_i\bar{F}_2}H_L^{W^*F_1\bar{l}_i}\Big], \\
B_3^L(W) = &\sum_{F_1,F_2=\nu}-\frac{7}{2}\frac{m_{F_1}m_{F_2}}{e^2m_W^4}\frac{\partial}{\partial x_W}G_1(x_W,x_{F_1},x_{F_2})H_L^{Wl_j\bar{F}_1}H_L^{W^*F_2\bar{l}_i}H_L^{Wl_i\bar{F}_2}H_L^{W^*F_1\bar{l}_i}, \\
B_2^L(W) = &\,0, \quad B_4^L(W) = \frac{1}{14}B_3^L(W), \quad B_5^L(W) = -\frac{1}{7}B_3^L(W), \\
B_1^R(W) = &\,B_2^R(W) = 0, \quad B_t^R(W) = B_t^L(W), \quad t = 3,4,5.
\end{aligned} \tag{46}$$

With Eqs.(43,45,46), $B_\beta^{L,R}$ are expressed as

$$B_\beta^{L,R} = B_\beta^{L,R}(n) + B_\beta^{L,R}(c) + B_\beta^{L,R}(W), \quad (\beta = 1\ldots 5)\,. \tag{47}$$

The decay widths for $l_j \to 3l_i$ can be computed from the front amplitudes,

$$\begin{aligned}
\Gamma(l_j \to 3l_i) = {} & \frac{e^4}{512\pi^3} m_{l_j}^5 \Big\{ \big(\big|C_2^L\big|^2 + \big|C_2^R\big|^2 \big) \big(\frac{16}{3} \ln \frac{m_{l_j}}{2m_{l_i}} - \frac{14}{9} \big) \\
& + \big(\big|C_1^L\big|^2 + \big|C_1^R\big|^2 \big) - 2 (C_1^L C_2^{R*} + C_2^L C_1^{R*} + \text{H.c.}) + \frac{1}{6} \big(\big|B_1^L\big|^2 + \big|B_1^R\big|^2 \big) \\
& + \frac{1}{3} \big(\big|B_2^L\big|^2 + \big|B_2^R\big|^2 \big) + \frac{1}{24} \big(\big|B_3^L\big|^2 + \big|B_3^R\big|^2 \big) + 6 \big(\big|B_4^L\big|^2 + \big|B_4^R\big|^2 \big) \\
& + \frac{1}{12} \big(\big|B_5^L\big|^2 + \big|B_5^R\big|^2 \big) - \frac{1}{6} (B_2^L B_5^{L*} + B_2^R B_5^{R*} + C_1^L B_5^{L*} + C_1^R B_5^{R*} + \text{H.c.}) \\
& + \frac{1}{3} (C_2^R B_5^{L*} + C_2^L B_5^{R*} + \text{H.c.}) - \frac{1}{6} (N_{LR} B_5^{L*} + N_{RL} B_5^{R*} + \text{H.c.}) \\
& - \frac{1}{2} (B_3^L B_4^{L*} + B_3^R B_4^{R*} + \text{H.c.}) + \frac{1}{3} (C_1^L B_1^{L*} + C_1^R B_1^{R*} + C_1^L B_2^{L*} \\
& + C_1^R B_2^{R*} + \text{H.c.}) - \frac{2}{3} (C_2^R B_1^{L*} + C_2^L B_1^{R*} + C_2^L B_2^{R*} + C_2^R B_2^{L*} + \text{H.c.}) \\
& + \frac{1}{3} \Big[2 (|N_{LL}|^2 + |N_{RR}|^2) + (|N_{LR}|^2 + |N_{RL}|^2) + (B_1^L N_{LL}^* + B_1^R N_{RR}^* \\
& + B_2^L N_{LR}^* + B_2^R N_{RL}^* + \text{H.c.}) + 2 (C_1^L N_{LL}^* + C_1^R N_{RR}^* + \text{H.c.}) \\
& + (C_1^L N_{LR}^* + C_1^R N_{RL}^* + \text{H.c.}) - 4 (C_2^R N_{LL}^* + C_2^L N_{RR}^* + \text{H.c.}) \\
& - 2 (C_2^L N_{RL}^* + C_2^R N_{LR}^* + \text{H.c.}) \Big] \Big\},
\end{aligned} \tag{48}$$

with

$$\begin{aligned}
& N_{LL} = \frac{N_L H_L^{Z l_i \bar{l}_i}}{m_Z^2}, \qquad N_{RR} = N_{LL} \,|_{L \leftrightarrow R} \,, \\
& N_{LR} = \frac{N_L H_R^{Z l_i \bar{l}_i}}{m_Z^2}, \qquad N_{RL} = N_{LR} \,|_{L \leftrightarrow R} \,.
\end{aligned} \tag{49}$$

With the fomula $\frac{\Gamma(l_j \to 3l_i)}{\Gamma(l_j)}$, the branching ratios of $l_j \to 3l_i$ are obtained.

IV. NUMERICAL RESULTS

In this section we discuss the numerical results, and consider the experiment constraints from the lightest neutral CP-even Higgs mass $m_{h^0} \simeq 125.7$ GeV [19] and the neutrino experiment data. In this model, the neutron EDM, lepton EDM and muon MDM are studied in our previous works, and their constraints are also taken into account. In this work, we use the parameters[21] $L_4 = \frac{3}{2}, \lambda_{N^c} = 1$. The Yukawa couplings of neutrinos $(Y_\nu)^{IJ}, (I, J = 1, 2, 3)$ are at the order of $10^{-8} \sim 10^{-6}$, whose effects to the CLFV processes are tiny and can be ignored.

To simplify the numerical discussion, we use the following relations

$$(A_l)_{ii} = AL, \quad (A_{N^c})_{ii} = (A_N)_{ii} = AN, \quad (A'_l)_{ii} = A'_L,$$
$$(m^2_{\tilde{N}^c})_{ii} = M^2_{sn}, \quad (m^2_{\tilde{L}})_{ii} = (m^2_{\tilde{R}})_{ii} = s^2_m, \quad \texttt{for} \;\; i = 1, 2, 3. \tag{50}$$

If we do not specially declare, the non-diagonal elements of the used parameters should be zero.

A. $l_j \to l_i + \gamma$

Charged lepton flavor violation is related to the new physics, and the branching ratio of the process $\mu \to e + \gamma$ is strict. Its experiment upper bound is 5.7×10^{-13} at 90% confidence level. At this subsection, the supposed parameters are $AN = -500\text{GeV}, m_L = 3\text{TeV}$.

1. $\mu \to e + \gamma$

With the parameters $M_{sn} = 1\text{TeV}, \mu_L = 1\text{TeV}, g_L = 1/6, v_{L_t} = 3\text{TeV}, \tan\beta_L = 2$, we numerically study the CLFV process $\mu \to e + \gamma$. The mass matrix of neutralino includes m_1 and m_2. m_2 is also related with the mass matrix of chargino. Therefore, the two parameters m_1 and m_2 can effect the contributions(neutalino-slepton, chargino-sneutrino) for $\mu \to e + \gamma$ to some extent. Supposing $\mu_H = 480\text{GeV}, \tan\beta = 11, s_m = 3400\text{GeV}, AL = -2\text{TeV}, A'_L = 300\text{GeV}$, we scan the parameters of m_1 versus m_2 in Fig.4. It implies that in this condition m_1 should be in the region $(430 \sim 630)$GeV and the effects of m_2 are small.

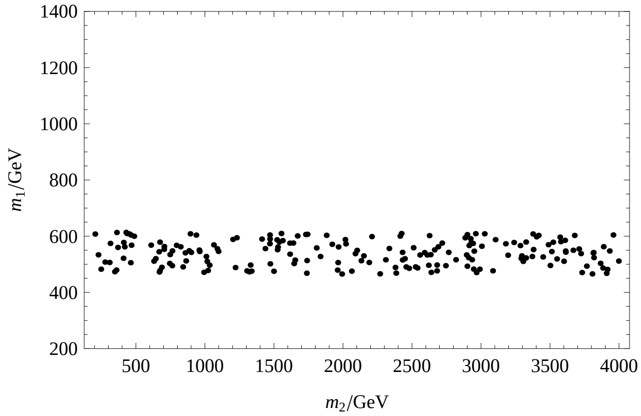

FIG. 4: For $\mu \to e + \gamma$, the allowed parameters in the plane of m_1 versus m_2 with $\mu_H = 480\text{GeV}, \tan\beta = 11, s_m = 3400\text{GeV}, AL = -2\text{TeV}, A'_L = 300\text{GeV}$.

The slepton mass squared matrix has A'_L and AL as non-diagonal elements which affect the results through slepton-neutralino and slepton-lepton neutralino contributions. With $\mu_H = 480\text{GeV}, \tan\beta = 12, s_m = 3300\text{GeV}, m_1 = 500\text{GeV}, m_2 = 1\text{TeV}$, in Fig.5 A'_L versus AL are scanned. Fig.5 shows that the effects from AL are smaller than the effects from A'_L. The allowed region of A'_L is about $(-2 \sim 2)$TeV.

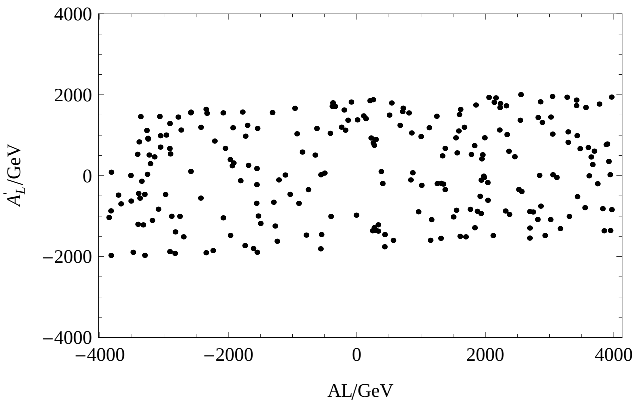

FIG. 5: For $\mu \to e + \gamma$, the allowed parameters in the plane of AL versus A'_L with $\mu_H = 480\text{GeV}, \tan\beta = 12, s_m = 3300\text{GeV}, m_1 = 500\text{GeV}, m_2 = 1\text{TeV}$.

$\tan\beta$ is related to the mass matrices of chargino, neutralino, slepton and sneutrino, especially to the non-diagonal elements of these matrices. In BLMSSM, almost all contributions to CLFV processes are influenced by $\tan\beta$. It is a sensitive parameter and affects the numerical results forcefully. $m^2_{\tilde{L}}$ and $m^2_{\tilde{R}}$ are introduced in the soft breaking terms. Both slepton and sneutrino mass squared matrices include $m^2_{\tilde{L}}$ and $m^2_{\tilde{R}}$, which should give considerable effects to CLFV processes. Supposing $\mu_H = 470\text{GeV}, m_1 = 500\text{GeV}, m_2 = 1\text{TeV}, AL = -2\text{TeV}, A'_L = 300\text{GeV}$, we plot the results with the allowed $\tan\beta$ versus s_m in Fig.6. As we expected, they both are sensitive parameters. Because the upper bound of $Br(\mu \to e + \gamma)$ is small, it is easy to exceed the bound in BLMSSM with the new contributions.

2. $\tau \to e + \gamma$

The experiment upper bound of $Br(\tau \to e + \gamma)$ is 3.3×10^{-8} which is almost five-order larger than that of $Br(\mu \to e + \gamma)$. Here we use the parameters $m_2 = 1\text{TeV}, \tan\beta_L = 2, M_{sn} = 2\text{TeV}, AL = -2\text{TeV}, A'_L = 300\text{GeV}, \mu_L = 1\text{TeV}, g_L = \frac{1}{6}$ and $v_{L_t} = 3\text{TeV}$. As discussed in the previous part, s_m can affect the contributions strong through slepton masses. Both slepton-neutralino and slepton-lepton neutralino give one loop corrections to the CLFV processes. Using the parameters $m_1 = 600\text{GeV}, \mu_H = 700\text{GeV}$ and $\tan\beta = 10(15, 25)$ in Fig.(7) we plot the results varying with s_m by the dashed line, dotted line and solid

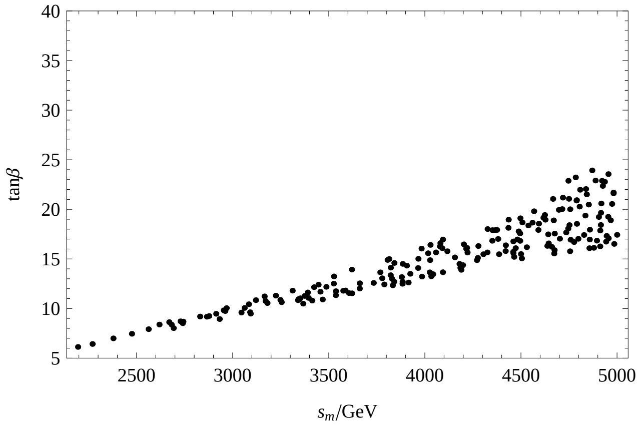

FIG. 6: For $\mu \to e + \gamma$, the allowed parameters in the plane of $\tan\beta$ versus s_m with $\mu_H = 470\text{GeV}, m_1 = 500\text{GeV}, m_2 = 1\text{TeV}, AL = -2\text{TeV}, A'_L = 300\text{GeV}$.

line. These three lines are all decreasing functions of the enlarging s_m. In the s_m region $(1000 \sim 1500)$GeV, the dashed line varies from 1.0×10^{-8} to 1.0×10^{-9}; the solid line varies from 1.0×10^{-7} to 1.0×10^{-8}. As $s_m > 2500$GeV, the three lines are all much smaller than the upper bound. Corresponding to same s_m during the region $(1 \sim 2)$TeV, the solid line results are about 10 times as the dashed line results, and the dotted line results are about 3 times as the dashed line results. It implies that both s_m and $\tan\beta$ are sensitive parameters to the numerical results. Larger $\tan\beta$ leads to larger results obviously.

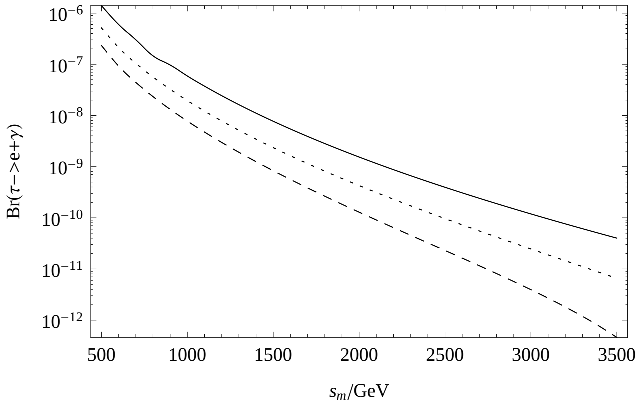

FIG. 7: With $\tan\beta = 10(15, 25)$, the results of $Br(\tau \to e + \gamma)$ versus s_m are plotted by the dashed line, dotted line and solid line respectively.

μ_H is included in the mass matrices of chargino and neutralino, which should produce considerable influence on the numerical results. With small $\tan\beta$ and large s_m, the results for $\tau \to e + \gamma$ are much smaller than the experiment upper bound. To embody effects from

μ_H and m_1, we use large $\tan\beta = 25$ and small $s_m = 800\text{GeV}$. The allowed numerical results are plotted by the dots in the Fig.8.

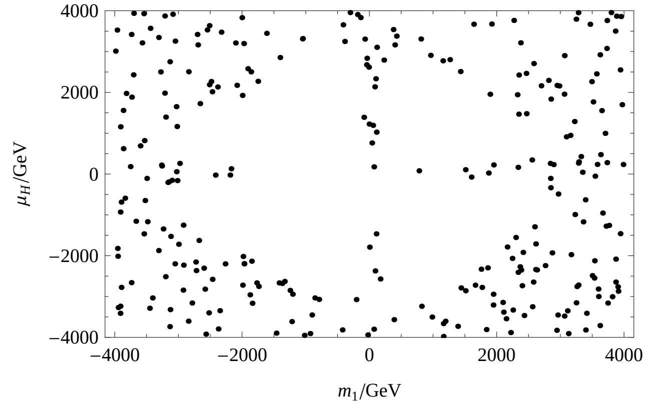

FIG. 8: For $\tau \to e + \gamma$, the allowed parameters in the plane of μ_H versus m_1 with $s_m = 800\text{GeV}, \tan\beta = 25$.

The non-diagonal elements of $(m^2_{\tilde{L}})$ and $(m^2_{\tilde{R}})$ represent the lepton flavor mixing and lead to strong mixing for sleptons (sneutrinos). To simplify the discussion, the assumption $(m^2_{\tilde{L}})_{ij} = (m^2_{\tilde{R}})_{ij} = ML_f$ for $i \neq j$ and $i, j = 1, 2, 3$ is used. We also consider the non-diagonal elements of A_l with the supposition $(A_l)_{ij} = A_f$ for $i \neq j$ and $i, j = 1, 2, 3$. Using the parameters $\mu_H = 480\text{GeV}, m_1 = 800\text{GeV}, s_m = 1500\text{GeV}, \tan\beta = 15$, in the plane of ML_f versus A_f the parameter space is scanned, and the allowed results are shown in Fig.9. The effects from ML_f are stronger than the effects from A_f. Here, the allowed region for ML_f is about $(-4 \times 10^5 \sim 8 \times 10^5)$ GeV^2.

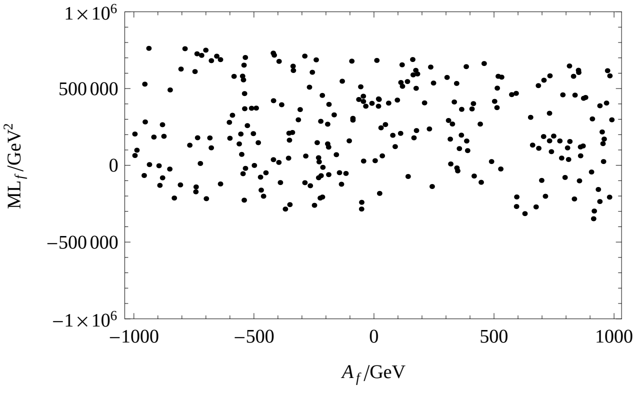

FIG. 9: For $\tau \to e + \gamma$, the allowed parameters in the plane of ML_f versus A_f with $\mu_H = 480\text{GeV}, m_1 = 800\text{GeV}, s_m = 1500\text{GeV}, \tan\beta = 15$.

3. $\tau \to \mu + \gamma$

Similar as $\tau \to e + \gamma$, the branching ratio of $\tau \to \mu + \gamma$ is also large, whose experiment upper bound is 4.4×10^{-8}. For the decay $\tau \to \mu + \gamma$, the parameters $m_2 = 1\text{TeV}, \mu_H = 500\text{GeV}, m_1 = 800\text{GeV}, M_{sn} = 2\text{TeV}, AL = -2\text{TeV}, s_m = 1\text{TeV}, A_L' = 300\text{GeV}$ are used. The gaugino mass m_1 is related to the neutralino-slepton contributions to CLFV processes. With $\tan\beta = 15$, $\mu_H = 500(1500, 3000)\text{GeV}$, in Fig.(10) the results of $Br(\tau \to \mu + \gamma)$ are studied versus m_1 by the dashed line, dotted line and solid line. As $|m_1|$ is around 600GeV, these three lines arrive at their big values. The results are decreasing functions of the increasing $|m_1|$, when $|m_1|$ is larger than 800 GeV. The biggest value of the dashed line can reach 3.2×10^{-8}. The solid line varies from 1.0×10^{-10} to 5.1×10^{-9}. The dashed line is the highest line and the solid line is the lowest one. The dotted line is the middle line and at the order of 10^{-8}. The three lines show the CLFV processes are suppressed by heavy virtual particles at several TeV order.

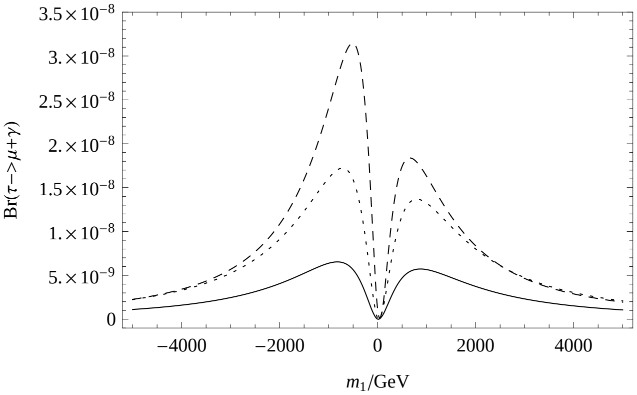

FIG. 10: With $\mu_H = 500(1500, 3000)\text{GeV}$, the results of $Br(\tau \to \mu + \gamma)$ versus m_1 are plotted by the dashed line, dotted line and solid line respectively.

Compared with MSSM, $\tan\beta_L$ and v_{L_t} are new parameters that have relation with mass matrices of slepton, sneutrino and lepton neutralino. Therefore, the effects to CLFV process $\tau \to \mu + \gamma$ from $\tan\beta_L$ and v_{L_t} are of interest. Based on the supposition $g_L = \frac{1}{6}, \mu_L = 1\text{TeV}, \tan\beta = 18$, we scan the parameter space of $\tan\beta_L$ versus v_{L_t} in Fig.11. The value of $\tan\beta_L$ can vary from $(0 \sim 40)$, whose effects are small. As $\tan\beta_L > 2.0$, v_{L_t} should be no more than 3600 GeV.

g_L is not only the coupling constant for lepton neutralino-slepton-lepton but also constitute the mass matrix of lepton neutralino. Considerable influence to $\tau \to \mu + \gamma$ from

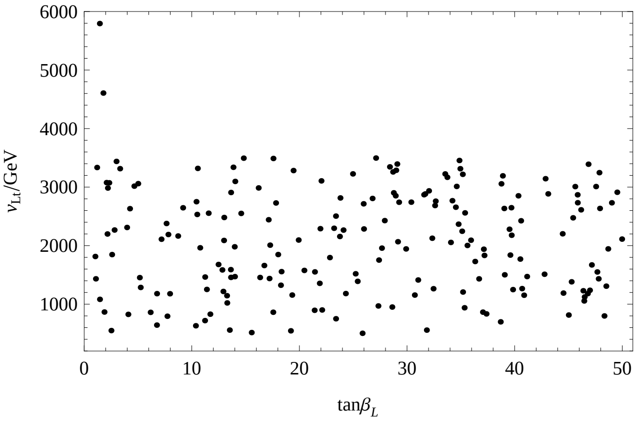

FIG. 11: For $\tau \to \mu + \gamma$, the allowed parameters in the plane of $\tan\beta_L$ versus v_{Lt} with $g_L = \frac{1}{6}, \mu_L = 1\text{TeV}, \tan\beta = 18$.

g_L is hopeful. The new gaugino mass μ_L is the non-diagonal element of the lepton neutralino mass matrix. To see how g_L and μ_L affect the numerical results for $\tau \to \mu + \gamma$, with $\tan\beta_L = 2, v_{L_t} = 3\text{TeV}, \tan\beta = 18$ we give out the allowed dots in the plane of g_L versus μ_L. Fig.12 implies that when g_L is near 0.5, the results are larger than the experiment upper bound. The effects from μ_L is very weak, and can be neglected.

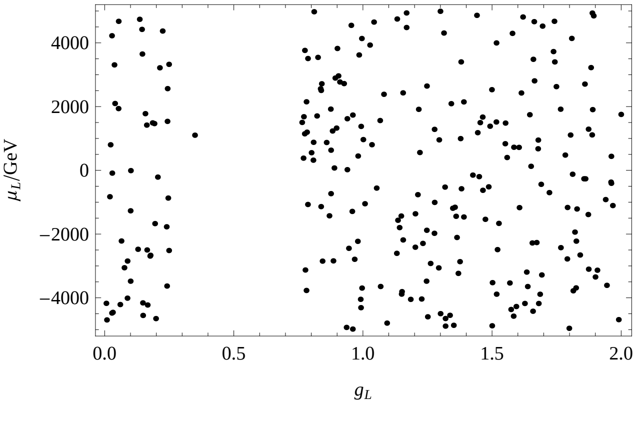

FIG. 12: For $\tau \to \mu + \gamma$, the allowed parameters in the plane of g_L versus μ_L with $\tan\beta_L = 2, v_{L_t} = 3\text{TeV}, \tan\beta = 18$.

B. $l_j \to 3l_i$

In this subsection, we numerically study the CLFV processes $l_j \to 3l_i$ with the supposed parameters $m_L = 3\text{TeV}, \mu_L = 1\text{TeV}, v_{L_t} = 3\text{TeV}$. These processes have close relations to

$l_j \to l_i + \gamma$.

1. $\mu \to 3e$

The most strict branching ratio of CLFV processes $l_j \to 3l_i$ is $Br(\mu \to 3e)$, whose experiment upper bound is 1.0×10^{-12}. This experiment constraint is the first one to be considered for $l_j \to 3l_i$. To study the process $\mu \to 3e$, the used parameters are $M_{sn} = 1\text{TeV}, s_m = 3300\text{GeV}, AN = -500\text{GeV}, AL = -2\text{TeV}, A_L' = 300\text{GeV}, m_1 = 500\text{GeV}, g_L = 1/6, \tan\beta_L = 2$. From the discussion in the front section, $\tan\beta$ and non-diagonal elements of $(m^2_{\tilde{L}})$ and $(m^2_{\tilde{R}})$ are sensitive parameters to the CLFV processes. With $\mu_H = 500\text{GeV}$ and $m_2 = 1500\text{GeV}$, the parameters $\tan\beta$ versus ML_f are scanned in the Fig.13. The plotted dots represent the allowed results which embody the influences from $\tan\beta$ and ML_f. Here, the value of $\tan\beta$ should be no more than 15.

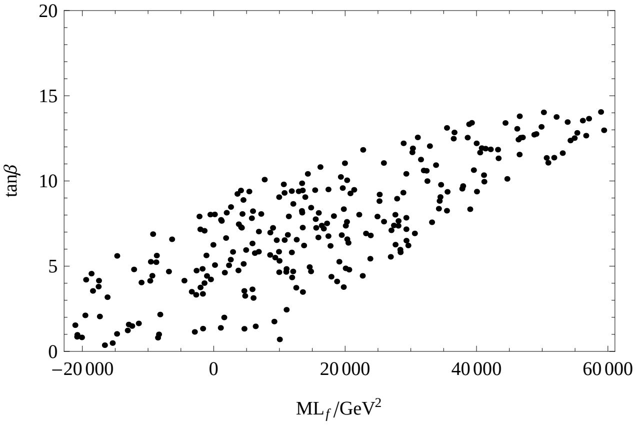

FIG. 13: For $\mu \to 3e$, the allowed parameters in the plane of $\tan\beta$ versus ML_f with $\mu_H = 500\text{GeV}, m_2 = 1500\text{GeV}$.

Here we consider the non-diagonal elements of $(m^2_{\tilde{L}})$ and $(m^2_{\tilde{R}})$, and suppose $ML_f = 10^4\text{GeV}^2$ and $\tan\beta = 10$. After the numerical calculation, the allowed parameters in the plane of m_2 versus μ_H are shown in the Fig.14. When μ_H is near 500 GeV, m_2 can vary from -3 TeV to 3 TeV. As $\mu_H > 600$ GeV, the allowed scope of m_2 shrinks with the enlarging μ_H.

2. $\tau \to 3e$

The experiment upper bound of the CLFV process $Br(\tau \to 3e)$ is (2.7×10^{-8}), and it is about four order larger than that of $\mu \to 3e$. For the study of $\tau \to 3e$, $\tan\beta = 10, M_{sn} = 2\text{TeV}, \mu_H = 3\text{TeV}, m_2 = 1500\text{GeV}, m_1 = 2500\text{GeV}$ are supposed here. To show the importance of the non-MSSM contributions from lepton neutralino-selepton, we discuss

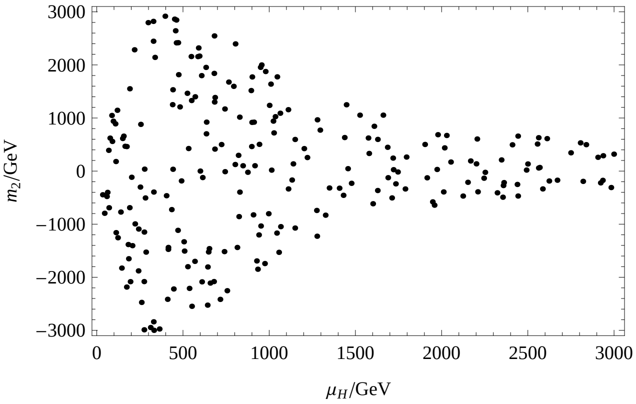

FIG. 14: For $\mu \to 3e$, the allowed parameters in the plane of m_2 versus μ_H with $ML_f = 10^4\text{GeV}^2, \tan\beta = 10$.

the effects from g_L and $\tan\beta_L$ with $s_m = 3500\text{GeV}, AN = -500\text{GeV}, AL = -2\text{TeV}, A_L^{'} = 300\text{GeV}$. Fig.15 implies in the g_L region $(0 \sim 2)$, the allowed scope of $\tan\beta_L$ is from 0 to 50. When g_L is larger than 2.2, the region of $\tan\beta_L$ turns very small which is just from 0 to 2.

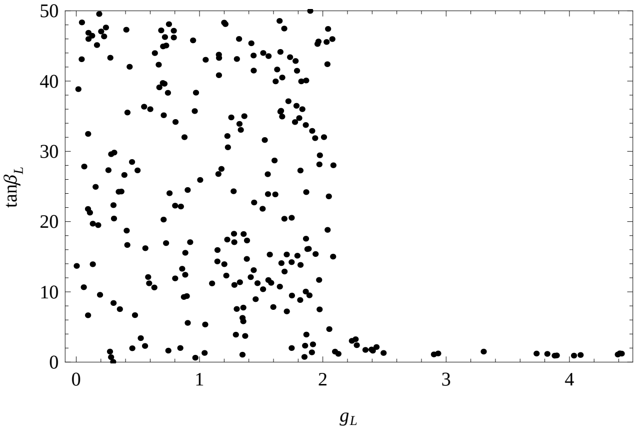

FIG. 15: For $\tau \to 3e$, the allowed parameters in the plane of $\tan\beta_L$ versus g_L with $s_m = 3500\text{GeV}, AN = -500\text{GeV}, AL = -2\text{TeV}, A_L^{'} = 300\text{GeV}$.

$(m_{\tilde{L}}^2)$ and $(m_{\tilde{R}}^2)$ are sensitive parameters relating to lepton mixing between different generations. That is to say, their diagonal and non-diagonal elements are all important factors for CLFV processes. As $AN = 2\text{TeV}, AL = 2\text{TeV}, A_L^{'} = 500\text{GeV}, g_L = 0.1, \tan\beta_L = 1$, the allowed scope of s_m versus ML_f is plotted in the Fig.16. ML_f should be no less than $-2.0 \times 10^5\text{GeV}^2$ and the allowed smallest values of ML_f turn large with the enlarging s_m.

3. $\tau \to 3\mu$

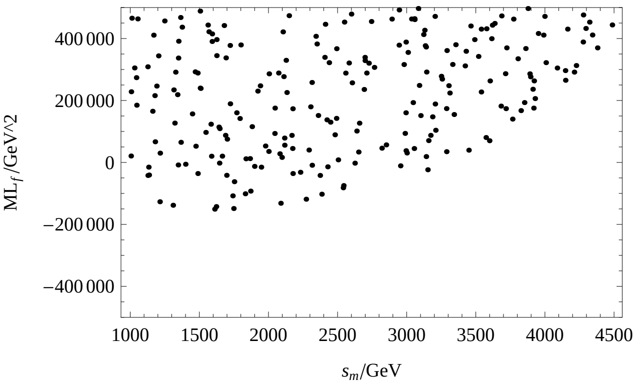

FIG. 16: For $\tau \to 3e$, the allowed parameters in the plane of s_m versus ML_f with $AN = 2\text{TeV}, AL = 2\text{TeV}, A_L^{'} = 500\text{GeV}, g_L = 0.1, \tan\beta_L = 1$.

Similarly, we calculate the CLFV process $\tau \to 3\mu$, whose experiment upper bound is $Br(\tau \to 3\mu) < 2.1 \times 10^{-8}$. To obtain the numerical results for $\tau \to 3\mu$, we use $M_{sn} = 1\text{TeV}, \mu_H = 500\text{GeV}, m_2 = 1500\text{GeV}, m_1 = 2500\text{GeV}, AN = 3\text{TeV}, AL = 3\text{TeV}, A_L^{'} = 3\text{TeV}, g_L = 0.4$. In the studied processes, there are two angles $\tan\beta$ and $\tan\beta_L$ relating to the contributions. In the plane of $\tan\beta$ versus $\tan\beta_L$, with $s_m = 1500\text{GeV}$ we show the allowed results denoted by the dots in Fig.17. The suitable value of $\tan\beta$ is in the region $(0 \sim 10)$. Compared with the effects from $\tan\beta$, those effects from $\tan\beta_L$ are tiny.

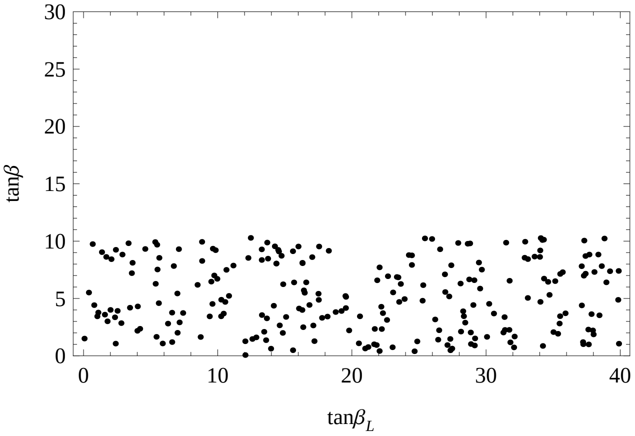

FIG. 17: For $\tau \to 3\mu$, the allowed parameters in the plane of $\tan\beta$ versus $\tan\beta_L$ with $s_m = 1500\text{GeV}$.

The mass squared matrix of sneutrino include A_N, A_{N^c} and $m^2_{\tilde{N}^c}$, which naturally influence the contributions from sneutrinos and charginos. We take into account the non-diagonal elements of these parameters and suppose $(A_N)_{ij} = (A_{N^c})_{ij} = AN_f$, $(m^2_{\tilde{N}^c})_{ij} = MN_f$ for

$i \neq j$ and $i, j = 1, 2, 3$. With $\tan\beta = 10, \tan\beta_L = 10, s_m = 2\text{TeV}$, in Fig.18 we plot the allowed results in the plane of AN_f versus MN_f. To obtain the allowed results, AN_f is no more than zero. The effects from MN_f are tiny and ignorable.

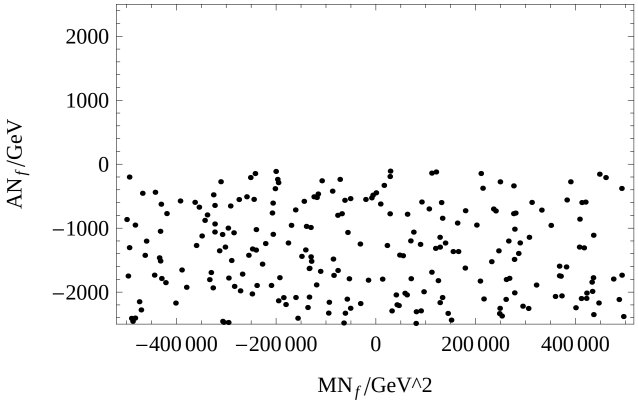

FIG. 18: For $\tau \to 3\mu$, the allowed parameters in the plane of AN_f versus MN_f with $\tan\beta = 10, \tan\beta_L = 10, s_m = 2\text{TeV}$.

V. DISCUSSION AND CONCLUSION

In SM the theoretical predictions for CLFV processes $l_j \to l_i + \gamma$ and $l_j \to 3l_i$ are much smaller than their experiment upper bounds. If large branching ratios of CLFV processes are detected, there must be new physics beyond SM. In BLMSSM, there are new parameters and new contributions to CLFV processes. For example, beside three light neutrinos there are three heavy neutrinos and six sneutrinos. Furthermore, new gauginos and new higgsinos mix leading to three lepton neutralinos, that can give new type contributions through the coupling of lepton neutralino-slepton-lepton.

The branching ratio experiment upper bounds of $\mu \to e + \gamma$ and $\mu \to 3e$ are strict and rigorously confine the parameter space. For the both processes, it is very easy to exceed their experiment upper bounds. The experiment upper bounds of the processes $\tau \to e + \gamma, \tau \to \mu + \gamma, \tau \to 3e$ and $\tau \to 3\mu$ are all at the order of 10^{-8} and much larger than those of $\mu \to e + \gamma$ and $\mu \to 3e$. In our used parameter space of BLMSSM, the branching ratios of these six CLFV processes can be large enough to achieve the bounds and even surpass them. From the numerical results, one finds the important parameters are $\tan\beta, s_m, ML_f, m_1, m_2, \mu_H$ and g_L, where $\tan\beta, s_m, ML_f$ are very sensitive parameters. We hope in the near future large branching ratios of CLFV processes can be detected by the experiments.

Acknowledgements

This work has been supported by the Major Project of NNSFC(NO.11535002) and NNSFC(NO.11275036), the Open Project Program of State Key Laboratory of Theoretical Physics, Institute of Theoretical Physics, Chinese Academy of Sciences, China (No.Y5KF131CJ1), the Natural Science Foundation of Hebei province with Grant No. A2013201277, and the Found of Hebei province with the Grant NO. BR2-201 and the Natural Science Fund of Hebei University with Grants No. 2011JQ05 and No. 2012-242, Hebei Key Lab of Optic-Electronic Information and Materials, the midwest universities comprehensive strength promotion project.

[1] K. Abe et al.(T2K Collaboration), Phys. Rev. Lett. **107** (2011) 041801; J. Ahn et al. (RENO Collaboration), Phys. Rev. Lett. **108** (2012) 191802. , F.An et al. (DAYA-BAY Collaboration), Phys. Rev. Lett. **108** (2012) 171803.

[2] E. Ma, A. Natale, O. Popov, Phys. Lett. B**746** (2015) 114-116; I. Girardi , S.T. Petcov , A.V. Titov, Nucl. Phys. B **894** (2015) 733-768.

[3] P. Ghosh, S. Roy, JHEP **0904** (2009) 069; P. Ghosh, P. Dey, B. Mukhopadhyaya, S. Roy, JHEP **1005** (2010) 087.

[4] S. Petcov, Sov.J.Nucl.Phys. **25** (1977) 340.

[5] K.A. Olive et al. (Particle Data Group), Chin. Phys. C **38** (2014) 090001.

[6] T. Goto, Y. Okada, T. Shindou, M. Tanaka, R. Watanabe, Phys. Rev. D **91** (2015) 033007.

[7] J. Rosiek, Phys. Rev. D **41** (1990) 3464 [Erratum hep-ph/9511250].

[8] A. Ilakovac, A. Pilaftsis, L. Popov, Phys. Rev. D**87** (2013) 053014.

[9] J. Hisano, T. Moroi, K. Tobe, M. Yamaguchi, Phys. Rev. D **53** (1996) 2442.

[10] Hai-Bin Zhang, Tai-Fu Feng, Li-Na Kou, Shu-Min Zhao, Int.J.Mod.Phys. A **28** (2013) 24, 1350117; Hai-Bin Zhang, Tai-Fu Feng, Shu-Min Zhao, Tie-Jun Gao, Nucl.Phys. B **873** (2013) 300-324, Errutum: Nucl. Phys. B **879** (2014) 235.

[11] H.P. Nilles, Phys. Rep. **110** (1984) 1.

[12] P. F. Perez, Phys. Lett. B **711** (2012) 353; J. M. Arnold, P. F. Perez, B. Fornal, and S.

Spinner, Phys. Rev. D **85** (2012)115024.

[13] R. Barbieri, A. Masiero, Nucl. Phys. B **267** (1986) 679; S. Dimopoulos, L.J. Hall, Phys. Lett. B **207** (1987) 210.

[14] P. F. Perez and M. B. Wise, JHEP **1108** (2011) 068; Phys. Rev. D **82** (2010) 011901.

[15] Tai-Fu Feng, Shu-Min Zhao, Hai-Bin Zhang, et al., Nucl. Phys. B **871** (2013) 223.

[16] Shu-Min Zhao, Tai-Fu Feng, Ben Yan et al., JHEP **1310** (2013) 020.

[17] Shu-Min Zhao, Tai-Fu Feng, Xi-Jie Zhan, Hai-Bin Zhang, Ben Yan, JHEP **1507** (2015) 124.

[18] Fei Sun, Tai-Fu Feng, Shu-Min Zhao et al., Nucl. Phys. B **888** (2014) 30; . Tie-Jun Gao, Tai-Fu Feng, Fei Sun, Commun. Theor. Phys. **61** (2014) 1, 95-100; Fei Sun, Tai-Fu Feng , Tie-Jun Gao, Hai-Bin Zhang, Shu-Min Zhao, Int.J.Mod.Phys. A **29** (2014) 27, 1450153.

[19] CMS Collaboration, Phys. Lett. B **716** (2012) 30; ATLAS Collaboration, Phys. Lett. B **716** (2012) 1; CMS Collaboration arXiv:hep-ph/1301.3405.

[20] J.M. Arnold, P.F. Perez, B. Fornal, S. Spinner, Phys. Rev. D **85** (2012) 115024.

[21] Chen Biao, Zhao Shu-min, Yan Ben, et al., Commun. Theor. Phys. **61** (2014) 619-623; Shu-Min Zhao, Tai-Fu Feng, Hai-Bin Zhang et al., JHEP **1411** (2014) 119.